PLOS ONE

Development of a model estimating root length density from root impacts on a soil profile in pearl millet (*Pennisetum glaucum* (L.) R. Br). Application to measure root system response to water stress in field conditions

Awa Faye[1,2], Bassirou Sine[1,3], Jean-Louis Chopart[4], Alexandre Grondin[1,2,3,5], Mikael Lucas[1,2,5], Abdala Gamby Diedhiou[1,2,6], Pascal Gantet[5], Laurent Cournac[7,8], Doohong Min[9], Alain Audebert[1,3,10], Aboubacry Kane[1,2,6], Laurent Laplaze[1,2,5]*
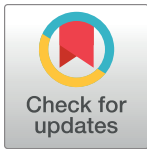
1 Laboratoire mixte international Adaptation des Plantes et microorganismes associés aux Stress Environnementaux (LAPSE), Dakar, Senegal, 2 Laboratoire Commun de Microbiologie, Dakar, Senegal, 3 Centre d'Etude Régional pour l'Amélioration de l'Adaptation à la Sécheresse, Institut Sénégalais de Recherches Agricoles, Thiès, Senegal, 4 Agerconsult, Montpellier, France, 5 UMR DIADE, Université de Montpellier, Institut de Recherche pour le Développement, Montpellier, France, 6 Département de Biologie Végétale, Université Cheikh Anta Diop, Dakar, Senegal, 7 UMR Eco&Sols, Université de Montpellier, Institut de Recherche pour le Développement, Centre de coopération Internationale en Recherche Agronomique pour le Développement, Institut National de la Recherche Agronomique, Montpellier Supagro, Montpellier, France, 8 Laboratoire mixte international Intensification Ecologique des Sols Cultivés en Afrique de l'Ouest (IESOL), Dakar, Senegal, 9 Department of Agronomy, Kansas State University, Manhattan, Kansas, United States of America, 10 UMR AGAP, Université de Montpellier, Centre de coopération Internationale en Recherche Agronomique pour le Développement, Institut National de la Recherche Agronomique, Montpellier SupAgro, Montpellier, France

* laurent.laplaze@ird.fr

Abstract

Pearl millet is able to withstand dry and hot conditions and plays an important role for food security in arid and semi-arid areas of Africa and India. However, low soil fertility and drought constrain pearl millet yield. One target to address these constraints through agricultural practices or breeding is root system architecture. In this study, in order to easily phenotype the root system in field conditions, we developed a model to predict root length density (RLD) of pearl millet plants from root intersection densities (RID) counted on a trench profile in field conditions. We identified root orientation as an important parameter to improve the relationship between RID and RLD. Root orientation was notably found to depend on soil depth and to differ between thick roots (more anisotropic with depth) and fine roots (isotropic at all depths). We used our model to study pearl millet root system response to drought and showed that pearl millet reorients its root growth toward deeper soil layers that retain more water in these conditions. Overall, this model opens ways for the characterization of the impact of environmental factors and management practices on pearl millet root system development.

Introduction

Pearl millet (*Pennisetum glaucum* (L.) R. Br., syn. *Cenchrus americanus* (L.) Morrone) is a cereal crop domesticated in the Western part of Sahel about 5,000 years ago [1]. It is well adapted to dry tropical climate and low-fertility soils and therefore plays an important role for food security in arid and semi-arid regions of sub-Saharan Africa and India. In these areas, pearl millet is an important source of nutritious food [2, 3] and is the staple crop for nearly 100 million people [4, 1]. Its grain is rich in protein (8–19%), essential micronutrients and calories [4]. It is also gluten-free and has hypoallergenic properties [4]. In a context of climate change leading to unpredictable weather patterns and rising temperatures in West Africa [5, 6], pearl millet could play an even more important role for food security because it can withstand hot and dry conditions that would lead to the failure of other locally grown cereal crops such as maize [4, 7]. However, pearl millet lags far behind other cereals in terms of breeding and its yield is low [4]. The recent sequencing of a reference genome and about 1, 000 accessions [4] open the way for a new era of genomic-based breeding in pearl millet [8]. However, this will depend on the availability of phenotyping methods to characterize and exploit the available genetic diversity and identify interesting target traits.

Drought and low soil fertility are among the most important factors limiting pearl millet yield [9]. The root system is responsible for water and nutrient uptake, and root system architecture is therefore a potential target in pearl millet breeding program to address these constraints. It is also an important trait to consider when analyzing the impact of agricultural practices. However, despite tremendous progress in the genetic characterization of root development, root system architecture phenotyping remains challenging particularly in agronomically-relevant field conditions. The root length density (total length of roots per unit of soil volume; RLD) is a key factor to estimate the soil volume explored by a root system and consequently the amount of water and nutrients available to the plant [10–15]. Therefore, RLD could be used to screen drought-tolerant varieties.

The aim of this study was to develop a technique to map RLD in pearl millet plants from simple measurements in field conditions. In order to do so, we analyzed the relationship between RLD and root intersection densities (number of roots intersecting a vertical plane per unit of surface; RID) counted on trench profiles. From this, we computed and experimentally validated a simple mathematical model linking RLD to RID. We then used this model to study the effect of drought stress on pearl millet root system architecture in two pearl millet varieties.

Materials and methods

Plant material

Four millet varieties were used for model calibration (Exp. 1): Souna3, Gawane, Thialack2 and SL87 (Table 1). Six varieties were tested for model validation (Exp. 2): Souna3 (common between Exp. 1 and Exp. 2), IBV8004, GB8735, ISMI9507, SL423, and SL28 (Table 1). Seeds were provided by the Institut Sénégalais de Recherches Agricoles (ISRA). The impact of water stress on pearl millet root system development was tested in a third experiment (Exp. 3) on SL28 (dual-purpose variety) and LCICMB1 (inbred line; [16]).

Field trials

Field trials were performed at the Centre National de Recherche Agronomique station (CNRA) of the ISRA in Bambey, Senegal (14.42˚N, 16.28˚W, altitude 17 m) in collaboration with and with the permission of the ISRA. Trials did not involve endangered or protected species.

Table 1. Pearl millet varieties used in this study.

Varieties	Origin	Cycle (days)	Genetic nature	Maximum height (cm)
Souna3	Senegal	85–95	Synthetic	240
Gawane	Senegal	85	Composite	250
Thialack2	Senegal	95	Composite	250
SL87	Senegal	56	Landrace	242
SL423	Senegal	54	Landrace	253
SL28	Senegal	56	Landrace	267
IBV8004	Senegal	75–85	Synthetic	220
GB8735	Niger	70	Improved population	150
ISMI9507	Senegal	58	Synthetic	220
LCICMB1	Nigeria	80	Inbred line	142

https://doi.org/10.1371/journal.pone.0214182.t001

Our objective was to develop a model that would be generic i.e. that can be used for all pearl millet varieties in different seasons and sites. We therefore designed our field trials to maximize the diversity of conditions (i.e. were performed on different seasons, with different varieties and in different plots) between calibration and validation as described thereafter. Exp. 1 was performed for model calibration during the rainy season 2016, Exp. 2 was performed in the dry season 2017 for model validation and Exp. 3 was performed in the dry season 2018 for response of pearl millet to a water stress. Exp. 2 and 3 were performed in the dry season in order to fully control the irrigation regime. Soil in the field trials was sandy and had the typical characteristics of the West Africa Sahelian soils in which pearl millet is grown (S1 Table). Each experiment was performed in a different location in the station. Tillage and chemical fertilization were applied as recommended for pearl millet [17]. Weeding was performed before planting and one week before root measurements. Shoot Agro-morphological characters were measured at the end of the cycle as previously described [17].

Exp. 1 and Exp. 2 were laid out in a randomized complete block design with four plots per variety, each with five rows of 4 m long with a spacing of 0.8 m between plants and rows. In Exp. 1, water was provided by rainfall and additional irrigation was provided when needed (S1 Fig). Water stress was quantified using the PROBE water balance model [18]. The water balance simulations showed a decrease in the daily actual evapotranspiration to maximum evapotranspiration (AET/MET) ratio at the end of the cycle (S1 Fig). In Exp. 2, field was irrigated twice a week until 70 days after sowing (DAS) and rainfall occurred at the end of the cycle (S1 Fig). The AET/MET ratio decreased only during the last days of cropping cycle (S1 Fig).

Exp. 3 was laid out in a randomized complete blocks design with split-plot into four blocks (corresponding to four replications), the whole plots were for the water regime and the split-plots were for the varieties. Plots consisted in four rows of 4 m long with 0.80 m between plants and rows. Thinning was done on eight days after emergence, at the rate of 2 plants per planting hole. In the well-watered plots (WW), irrigation was performed twice per week with 30 mm water per irrigation. This was calculated to cover the weekly average evapotranspiration of pearl millet (equivalent to 49 mm water / week in the dry season). In the drought stress plots (DS), a water stress was applied by withholding irrigation from 40 DAS for 32 days (S2 Fig) leading to a strong decrease in the AET/MET ratio (S2 Fig). At 72 DAS irrigation was resumed until the end of the growth cycle in addition with the first rain in June (S2 Fig). Field dry-down was monitored by measuring volumetric soil moisture to evaluate the fraction of transpirable soil water (FTSW) using Diviner probes (Sentek Pty Ltd) as previously described [17,19].

Root phenotyping

We adapted a method previously described to estimate the RLD from intersections between roots and the face of a soil trench profile (root intersection density or RID; [13–15,20,21]). Trench profiles were dug perpendicularly to the sowing rows and at two distances (30 then 10 cm) from the plant stalk base (Fig 1A). Three-sided incomplete steel cubes with 0,1 m sharpened edges facilitating penetration into the soil were used to sample soil cubes (Fig 1BC). The sampling device was pressed into open soil profile (trench profile) until its rear plane was aligned with the soil profile (Fig 1D) and then cut out of the soil to obtain a cube of soil (Fig 1E). A second sample was taken at the same depth and distance from the plant but with the open sides oriented in the opposite direction. Hence, the two samples gave us measurements on open soil planes for the six sides of a cube. Sampling was made at six depth levels ranging from 0.1 to 1.1 m and at two different dates (60 and 80 days after sowing, DAS) corresponding to flowering and seed filling stages. For each soil cube, the number of impacts (number of roots intersecting a plane, NI) on each side (transversal, longitudinal and horizontal; Fig 1B) was counted in the field immediately after sampling (Fig 1F; [13–15]). NI was then used to calculate root intersection densities (RID, number of impacts per surface area) for the three open sides (horizontal, vertical-transversal, vertical-longitudinal) of each soil cube. Thereafter, roots were washed out of the sampled soil cubes using a sieving conventional technique. Root lengths were measured for thick (d >1 mm) and fine roots (d < 1 mm) after scanning and analysis with WinRhizo (v 4, Regent Instruments, Inc, Quebec, Canada). Measurements were repeated four times per variety (384 cubes in total) and repeated measurements were averaged (i.e., same variety, same seeding rate, same date and same position).

The same protocol was used in the validation test, except that measurements were performed at four sampling dates (21, 40, 60 and 80 DAS) at eight soil depths ranging from 0.1 to 1.6 m. Measurements were repeated three times per variety (725 cubes in total). Soil samples containing less than three roots on one side of the cube were not considered as they did not permit the quantification of preferential root orientation [13].

Soil-root intersections (root impacts) on a trench profile were counted using a 5 cm mesh grid applied to the soil profile (Fig 1G; [22,23]). Root intersections were counted at two distances (30 then 10 cm) from the base of the stalks and until no more roots could be found on the vertical dimension of the trench-profile. Root counting was performed at two dates of the cropping cycle: at the beginning of a stress (44 DAS) and at the end of stress (72 DAS). At each date, four trench profiles were measured per variety.

Model construction and test

A model was developed to establish a relationship between root impacts (root intersection densities, RID) counted on the two vertical planes of the cubes (longitudinal, l, and transversal plane, t; Fig 1B) and the measured root length density ($RLD_{measured}$) in the corresponding soil samples. RLD of fine and thick roots were calculated ($RLD_{calculated}$) on the basis of RID measured in a vertical soil plane using a direct empirical relationship first, and then considering the root distribution (anisotropy, root preferential orientation (P) as proposed by Lang and Melhuish [24]). A vertical index (Pv) was calculated for the two vertical planes (l and t) using root counted on three faces of a soil cube (l, t and horizontal, h) as follow:

$$p_v = \frac{2 * RID_h}{RID_t + RID_l} \qquad (Eq\ 1)$$

If $P_v < 1$ or > 1, the roots have a parallel or perpendicular preferential orientation with respect to the reference vertical plane. Depending on whether the P_v is = , $>$ or $<$ to 1, three
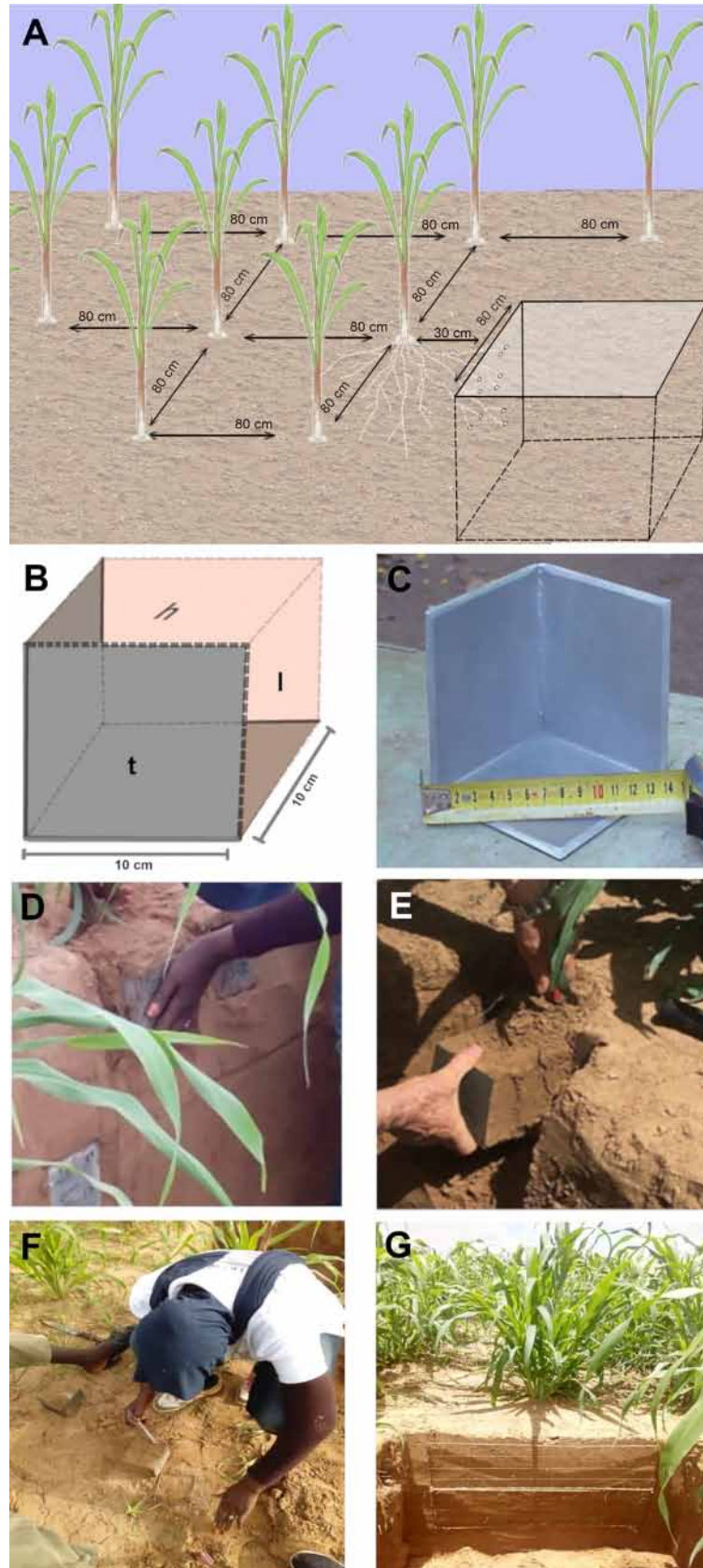
Fig 1. Root intersections density (RID) counting method used for root length density (RLD) modeling from RID.
(A) Experimental design and trench profile for root sampling (at 30 cm from the plant in this example), (B) and (C) sampling device with sides oriented according to the soil surface and plant row (H: horizontal, L: longitudinal, T: transversal), (D) and (E) root sampling process, (F) Root impacts counting on all three sides of soil cubes extracted from the trench profile, and (G) grid (5x 5 cm mesh) on a soil profile for soil-roots intersections counting (RI).

RLD equations can be considered (Eqs 2–4) to calculate RLD from RID on a vertical plane as previously shown [13–15,21,25]. They can be combined in a general relationship using a synthetic root orientation coefficient (CO) dependent on P_v index values as described in Eq 3:

$$\text{For Pv} > 1 : \quad RLD = \frac{RID(16P_v{}^2 + 2P_v + 1)}{(10P_v + 5)} \tag{Eq 2}$$

$$\text{For Pv} < 1 : \quad RLD = \frac{RID(3P_v{}^2 + 2P_v + 1)}{(2P_v} + 1) \tag{Eq 3}$$

$$\text{For Pv} = 1 \ (\text{isotropic distribution}) : \quad RLD = 2 * RID \tag{Eq 4}$$

$$RLD = RID * CO \tag{Eq 5}$$

with RID as number of impacts per m^2 and RLD expressed in m per m^3.

Statistical analyses

Excel 2013 (Microsoft Corporation) was used for data cleaning and synthesis, to calculate anisotropy and preferential orientation indexes and to develop and test the obtained models. SPSS and R softwares (IBM Corp. Released 2016. IBM SPSS Statistics for Windows, Version 24.0. Armonk, NY: IBM Corp and R Development Core Team (2008). URL http://www.R-project.org.) were used to study the relationships linking the direction indexes and the experimental factors through an analysis of variance and a Student's independence test at the 5% threshold.

The quality of the relationships between the RLD values measured in soil cubes (RLD$_m$) and those calculated using our models (RLD$_c$) were evaluated taking into account slope, intercept and regression (R^2). Four different statistical tests were used to further analyze the performance of our models:

- The Nash–Sutcliffe efficiency index NE is a widely used and reliable statistic for assessing the goodness of fit of models [26]. It ranges from $-\infty$ to 1 with NE = 1 being the optimal value. Values between 0.0 and 1.0 are generally viewed as acceptable levels of performance, whereas values <0.0 indicates that the mean observed value is a better predictor than the simulated value, which indicates unacceptable performance. For the case of regression procedures (i.e. when the total sum of squares can be partitioned into error and regression components), the Nash–Sutcliffe efficiency is equivalent to the coefficient of determination (R^2), thus ranging between 0 and 1. NE was calculated as follow:

$$NE = \frac{\sum_{i=1}^{n}(RLDm_i - Mean(RLDm))^2 - \sum_{i=1}^{n}(RLDc_i - RLDm_i)^2}{\sum_{i=1}^{n}(RLDm_i - Mean(RLDm))^2}$$

where Mean(RLDm) and Mean(RLDc) are the average measured and calculated root length densities and n, the size of the sample studied;

- The Root Mean Square Error (RMSE) is a measure of the relative difference between values predicted by a model and the values actually observed [27]. If the predicted and observed responses are very close the RMSE will be small. If the predicted and true responses differ substantially at least for some observations the RMSE will be large. A value of zero would indicate a perfect fit [26]. It is expressed as a % with values < 10% considered as very good and values > 25% considered as poor. Normalizing the RMSE facilitates the comparison between datasets or models with different scales. We calculated a Normalized RMSE (NRMSE) as follow:

$$NRMSE = \frac{100}{\max(RLDm) - \min(RLDm)} \sqrt{\frac{\sum_{i=1}^{n}(RLDc_i - RLDm)^2}{n}}$$

Where max(RLDm) and min(RLDm) are the maximum and the minimum values of the observed values and n, the number of observations.

- The mean absolute error measures the average magnitude of the errors in a set of predictions, without considering their direction. If the absolute value is not taken (the signs of the errors are not removed), the average error becomes the Mean Bias Error (MB) and is usually intended to measure average model bias. MB can take negative values. Under these conditions, the models underestimate the expected values. We calculated a MB as follow:

$$MB = 100 \frac{\sum_{i=1}^{n}(RLDc_i - RLDm_i)}{nMean(RLDm)}$$

Both RMSE and MB range from 0 to ∞, lower values are better and indicate a good estimation of expected values.

- The index of agreement (d) is the ratio of the mean square error and the potential error (PE) multiplied by *n* (number of observations) and then subtracted from one [28]. The index of agreement varies from -1 to 1 with index values closer to 1 indicating that the modeled values have better agreement with the observations. The d-index overcomes the insensitivity of Nash-Sutcliffe efficiency *(NE)* and coefficient of determination *(R^2)* to differences in the observed and model simulated means and variances. It was calculated as follow:

$$d = 1.0 - \frac{\sum_{i=1}^{n}(|RLDc_i - RLDm_i|)}{\sum_{i=1}^{n}(|RLDm_i - Mean(RLDc)| + |RLDc_i - Mean(RLDc)|)}$$

Results

Relation between RLD and RID in pearl millet varieties in field conditions

Four pearl millet varieties were selected to create a model estimating root length densities in field conditions. We first analyzed the diversity of these four pearl millet varieties for root and shoot characters. There were significant differences in root length densities (RLD) and root
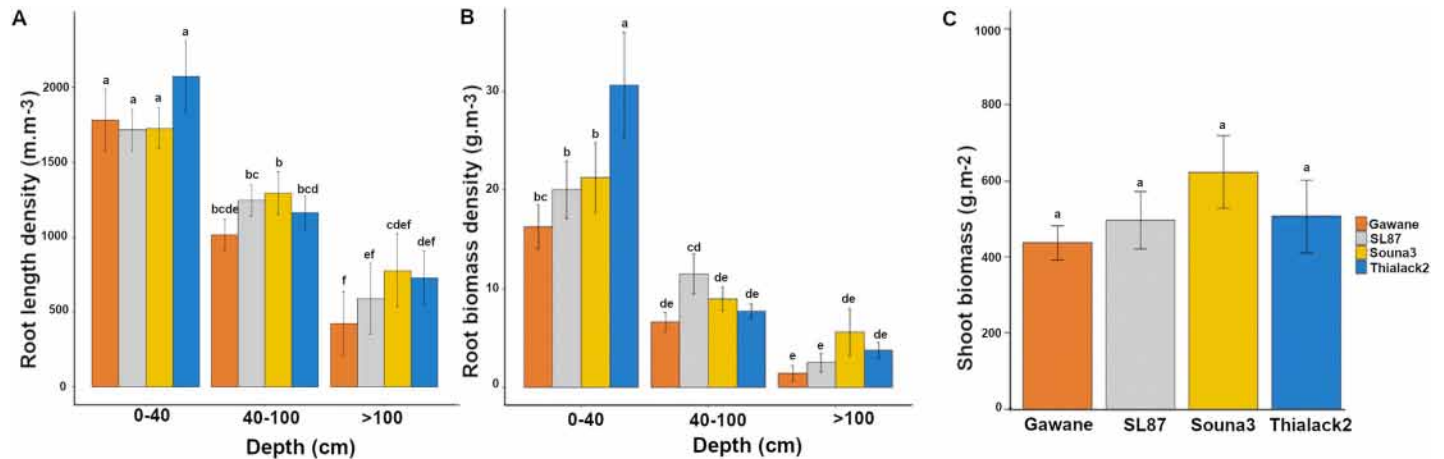
Fig 2. Characteristics of the varieties used for model calibration. (A) Root length density, (B) root biomass density and (C) shoot biomass. Data are mean +/- standard deviation. Significant differences (Tukey's HSD) are indicated by different letters. For root traits, the mean of the two observation dates (60 DAS and 80 DAS) was considered.

biomass densities (Fig 2A and 2B). Some varieties had deeper root systems than others. By contrast no significant differences were observed between varieties for shoot traits such as biomass (Fig 2C). Hence, these four varieties had contrasted root systems and were deemed suitable for model development.

We then analyzed the relationships between measured RLD and root intersection densities (i.e. the number of root impacts on a soil surface per surface unit; RID) on the vertical sides of a soil cube. The simple linear regression between RID in a vertical plane and RLD_m for all roots showed unsatisfactory fit (RLD = 1.83 RID; R^2 = 0.575, n = 70; Fig 3) indicating that more parameters needed to be included to estimate RLD from RID.

Development and calibration of models to estimate RLD from RID

In order to generate mathematical models linking RLD to RID, we estimated the importance of different parameters on the relation between these two parameters. We therefore analyzed the impact of soil depth (seven soil depths between 10 and 130 cm), plant varieties and distance to the plant stalk base on root growth orientation. The root preferential orientation on a vertical plane (P_v) was estimated from three-sided counts of a cube and used to calculate a root orientation coefficient (CO). We observed that the main root growth direction estimated by the P_v coefficient were not significantly different between varieties, measuring dates (60 DAS and 80 DAS) or sampling distances (10 or 30 cm; S2 Table). The P_v index only depended on depth. As a consequence, the results from all varieties, measurement dates and sampling distances were pooled and we only analyzed the relationship between depth and root growth orientation. Considering all roots, we found a linear relationship between the root orientation index on a vertical plane (P_v) and depth (Z in meters; Fig 4A; Pv = 0.3408 Z + 0.905; R^2 = 0.843, n = 70). Similarly, the root orientation coefficient (CO) was closely dependent on root depth (Fig 4B; B; CO = 0.471 Z +1.869; R^2 = 0.839, n = 70). CO values ranged from 1.92 at 0.10 m depth to 2.44 at 1.4 m depth. It was close to 2 close to the surface (0.10 m), indicating that roots had no preferential growth direction in the topsoil layers and that they gradually grew more in a vertical direction with depth.

The root direction coefficient of fine roots (CO) had a low dependence on soil depth (Fig 4A; COv = 0.089 Z+ 2.02; R^2 = 0.118, n = 70). P_v was close to 1 indicating a weak preferential
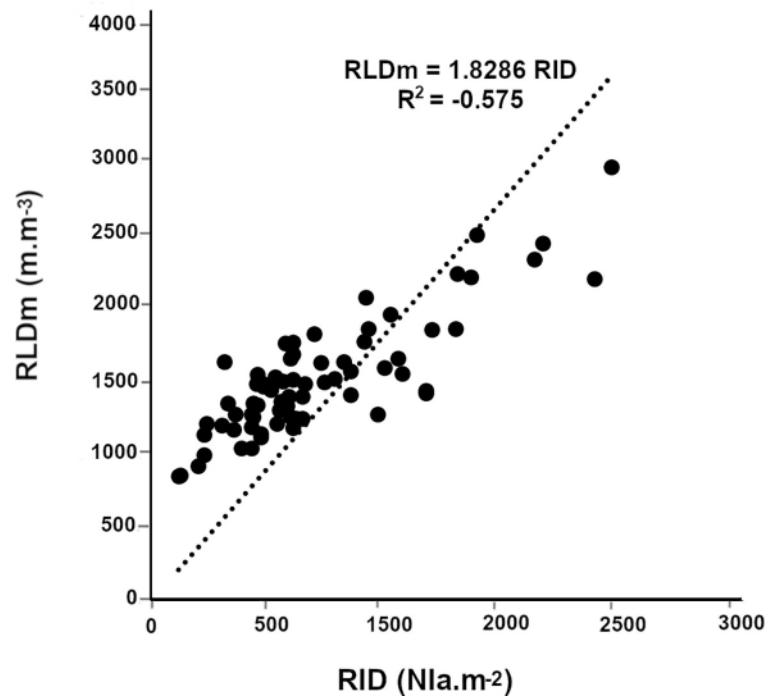
Fig 3. Fine and thick root growth orientation. Relationship between the number of measured root impacts on a vertical face and measured root length density.

direction of the fine roots. Similarly, CO had a low dependence on soil depth from 2.02 close to the surface to 2.18 at 1.1 meters depth (Fig 4B). For fine roots, we thus retained a fixed constant value of 2.08 corresponding to the average value of CO.

For thick roots, root direction (P_v) and root orientation coefficients (CO) were strongly dependent on soil depth (Fig 4; CO = 1.937 Z+1.42; R^2 = 0.839, n = 70). CO varied from 1.6 at 0.10 m depth to almost 4 at 1.3 m depth. This indicates that thick roots tend to grow horizontally close to the surface and that their growth becomes more and more vertical with soil depth.
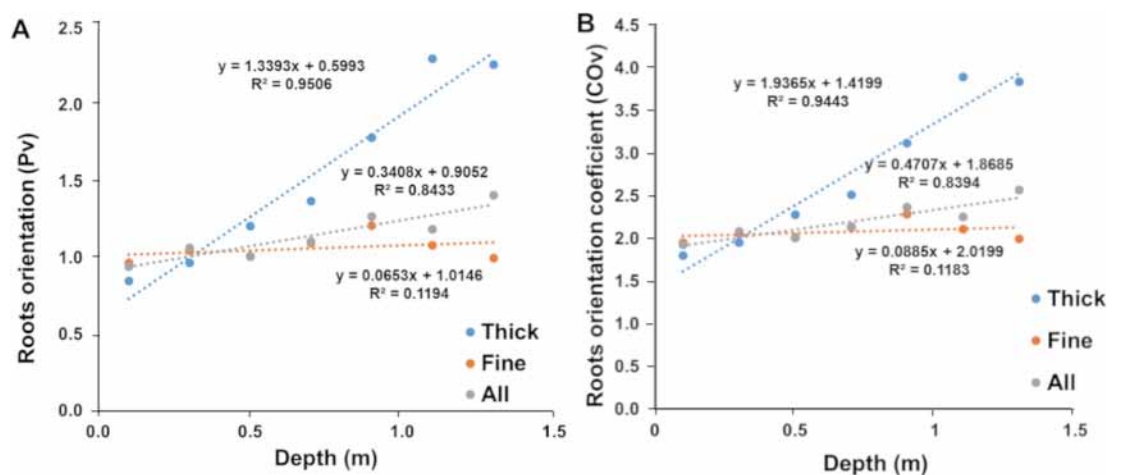

Fig 4. Elaboration of geometric models (all, thick and fine roots). Relationship between soil depth measurements (meters) and the main direction of root growth in relation to a vertical plane (Pv index).

Altogether, our results indicate that in field conditions pearl millet root orientation (and therefore the relation between RLD and RID) depends only on soil depth. Thick roots orientation is more sensitive to this than fine roots. We therefore included this information to build 4 models to estimate RLD from RID on the vertical plane taking soil depth (Z: depth in meter) into account:

- an empirical model for all roots: $RLD = 1.83{}^{*}RID$

- a geometrical model for all roots: $RLD = (0.471{}^{*}Z+1.87){}^{*}RID$

- a geometrical model for fine roots: $RLD = 2.08{}^{*}RID$

- a geometrical model for thick roots: $RLD = (1.937{}^{*}Z+1.42){}^{*}RID$

Models validation

Models developed from the data obtained on four varieties during the rainy season 2016 were tested during the dry season 2017 in another field location and with different varieties to maximize the differences between the calibration and validation tests. We used six varieties including five varieties different from those used for model calibration. The quality of the relationships obtained was studied taking into account slope, intercept and regression (R^2), Nash's Efficiency Ratio (NE; [26]), root mean square error (NRMSE; [27], mean bias error (MB) and d-index [27]. The results of our statistical tests on the different models are summarized in Table 2

There were good relationships between measured and calculated values for the model estimating only the fine roots (diameter < 1mm) for all varieties except GB 8735 (Fig 5A, Table 2).

RLD for thick roots (diameter > 1 mm) ranged from 0 to 2000 m.m^{-3}, about ten times lower (Fig 5B) than those for fine roots (Fig 5A). The model construction showed that when the impact density is very low, the relationship between the measured values and those calculated by the thick roots model becomes irregular (higher spread of values around the average) but there is no significant bias since the average values per depth of measured and calculated RLD were close (Fig 5D). However, the use of this model is limited by the low number of thick roots and the higher noise generated by the model for low RID.

Considering all roots (fine and thick), statistical tests showed that the measured and calculated RLD values were significantly closer with the geometrical model than with the empirical model (Table 2; Fig 5C and 5D).

Altogether, our experiments validated the geometrical model for RLD estimation from RID for all roots as the best model.

Response of pearl millet root system to water stress

We next used this model to study the effect of water stress on root architecture in two different pearl millet germplasms, the dual-purpose SL28 variety and the inbred line LCICMB1 (Exp. 3). These two germplasms were grown under irrigated conditions for 40 D. Irrigation was then stopped in the drought stress treatment for 31 days while it was maintained in the well-watered treatment. Irrigation was then resumed till the end of the cycle.

Soil water content was followed using Diviner probes and used to compute the fraction of transpirable soil water (FTSW) as previously described [17,19]. FSTW values below 40% indicate here water-limiting conditions [19]. In the well-watered treatment, FTSW remained above 40% along the soil profile from 30 to 90 DAS (S3 Fig). In the drought stress treatment, water withholding at 31 DAS led to soil drying and induced a reduction in FTSW that fall

Table 2. Models validation analyses.

Model	Root types	Variety	n	Slope	Intercept	R²	NRMSE (%)	MB (%)	NE	d
Empirical	All	All var	166	1.11	-1915	0.82	13	24	0.58	0.914
Geometrical	All	SL423	28	1.08	-1259	0.83	12	12	0.77	0.932
		Souna3	28	1.06	-1047	0.84	10	11.	0.79	0.938
		SL28	29	1.08	-1253	0.87	9	10	0.83	0.638
		IBV 8004	28	1.10	-1619	0.76	12	14	0.70	0.904
		GB 8735	25	1.41	-3345	0.88	13	11	0.78	0.918
		ISM 9507	28	1.07	-1064	0.73	12	8	0.71	0.905
		All var	166	1.11	-1491	0.81	9	11	0.77	0.926
Geometrical	Fine	SL423	28	1.12	-1229	0.80	12	10	0.76	0.924
		Souna3	28	1.11	-1228	0.84	11	11	0.80	0.973
		SL28	29	1.14	-1401	0.83	10	9	0.81	0.938
		IBV 8004	28	1.16	-1754	0.78	11	13	0.73	0.911
		GB 8735	25	1.52	-3464	0.89	13	8	0.78	0.913
		ISM 9507	28	1.13	-1282	0.72	13	7	0.70	0.897
		All var.	166	1.18	-1625	0.80	9	10	0.76	0.921
Geometrical	Thick	SL423	23	1.38	-223	0.64	16	-0.1	0.60	0.833
		Souna3	26	1.59	-269	0.75	17	-13	0.61	0.831
		SL28	26	1.21	-75	0.77	15	-9	0.73	0.905
		IBV 8004	21	0.77	169	0.33	21	-7	0.28	0.726
		GB 8735	18	0.97	60	0.32	26	-7	0.30	0.674
		ISM 9507	24	0.94	165	0.51	17	-22	0.41	0.811
		All var.	138	1.15	-30	0.59	13	-10	0.55	0.830

Characteristics of linear regressions between measured and calculated RLD values. Statistical tests on deviations between measured and calculated RLD values (NRMSE: normalized root mean square error), mean bias (MB) and Nash efficiency (NE) and the index of agreement (d).

under 40% between 50 DAS and 70 DAS in the 0–30 cm and 30–60 cm soil layers, respectively (S3 Fig). FTSW was also reduced in the 60–90 cm soil layer reaching 40% at 78 DAS, but remained above 40% below 90 cm throughout the drought stress treatment (S3 Fig). These results are consistent with the ETR / ETM crop ratio values calculated by water balance modeling that estimate ETR / ETM values below 0.3 between 60 and 75 DAS (S2 Fig). Altogether, these results indicate efficient field dry-down and imposition of water limited conditions from topsoil to a depth of around 90 cm in the drought stress treatment.

Agromorphological characteristics were then measured at the end of the cycle (99 DAS). SL28 is a dual-purpose pearl millet variety selected for both fodder and grain production. Accordingly, it shows a very large biomass and grain production compared to the inbred line LCICMB1 in well-watered conditions (Fig 6A and 6B). Moreover, these two lines showed contrasted responses to drought stress conditions. SL28 showed a very strong and significant reduction in both biomass and grain production in response to water stress while these traits were not significantly affected in LCICMB1 (Fig 6A and 6B).

We used the geometrical model for all roots to estimate RLD from RID along soil profiles. Measurements were performed in both well-watered and drought stress conditions for both lines at 43 and 71 DAS, i.e. at the beginning and at the end of the water stress period. Three days after stress application (43 DAS), the RLD profiles were not significantly different for well-watered and drought stress conditions for both lines (Fig 7A and 7B) indicating that the change in water availability had not significantly impacted root architecture at this stage.
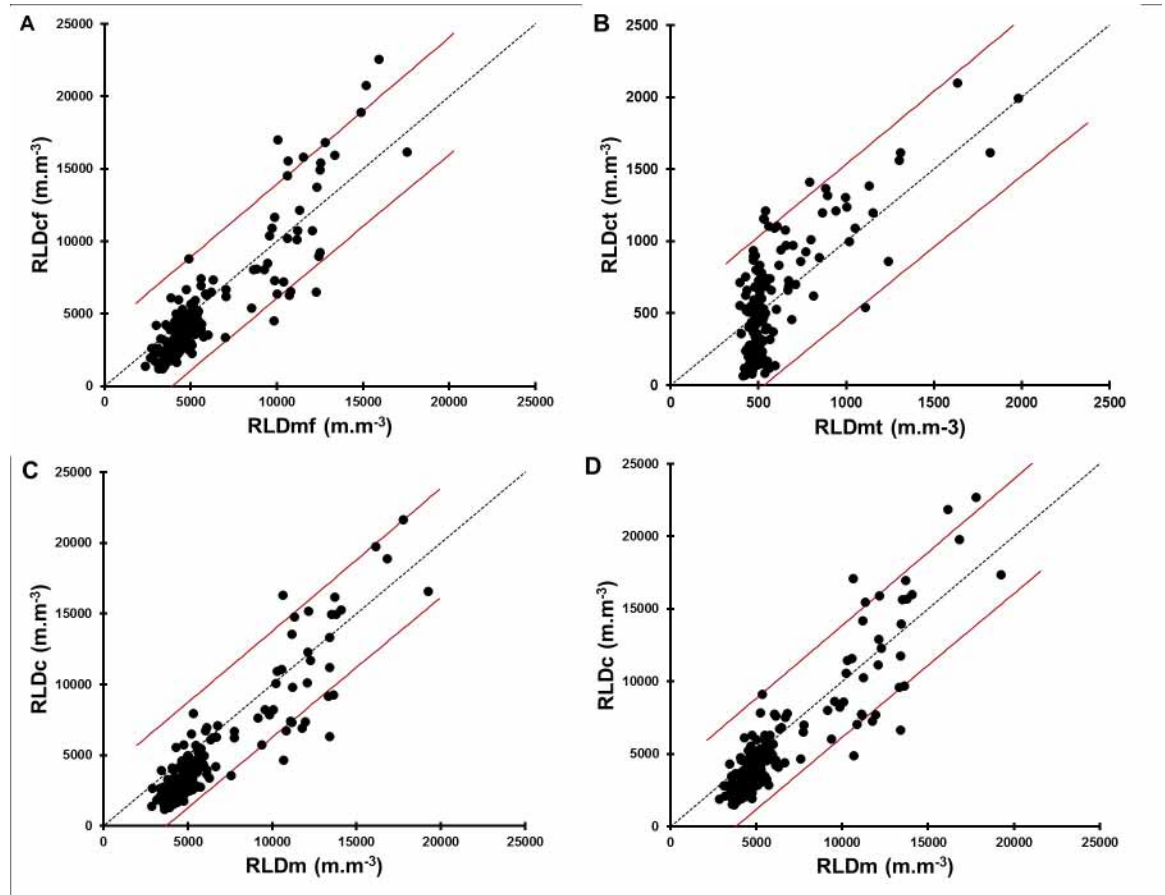
Fig 5. Test of the relationship between measured and calculated RLD for the four proposed models. (A) Geometrical models for fine roots (diameter<1 mm) and (B), thick roots (diameter >1 mm). (C) Empirical model with all varieties bulked and (D) geometrical model with all roots For all models, a prediction interval of 95% is indicated by the green lines. It gives an estimate of the interval in which a future observation will fall with a certain confidence level (here 95%), given previous observations used to build the model.
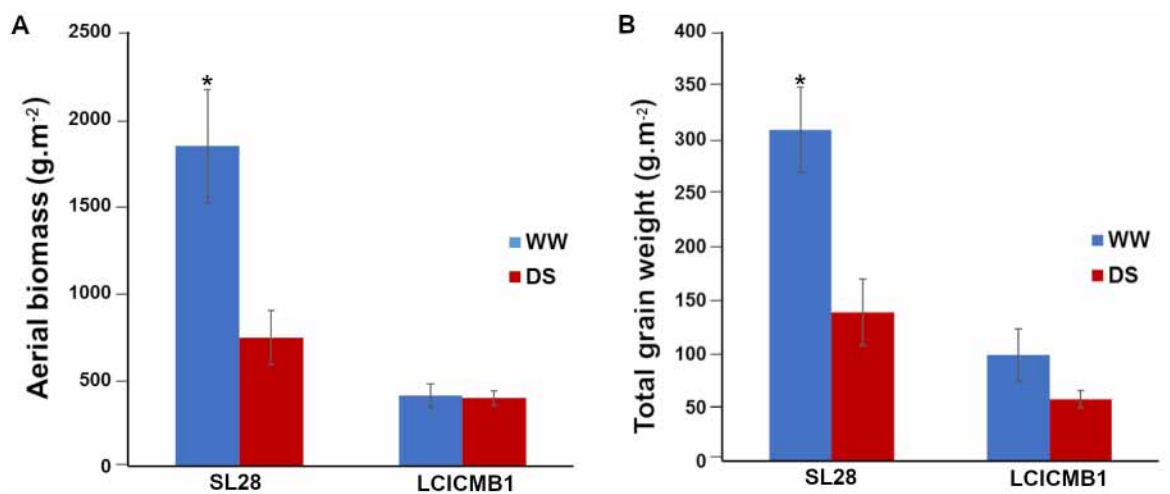
Fig 6. Agromorphological characteristics of SL28 and LCICMB1. (A) Shoot biomass (g.m^{-2}), and (B) total grain weight (g.m^{-2}) measured at the end of cycle for WW and DS conditions.
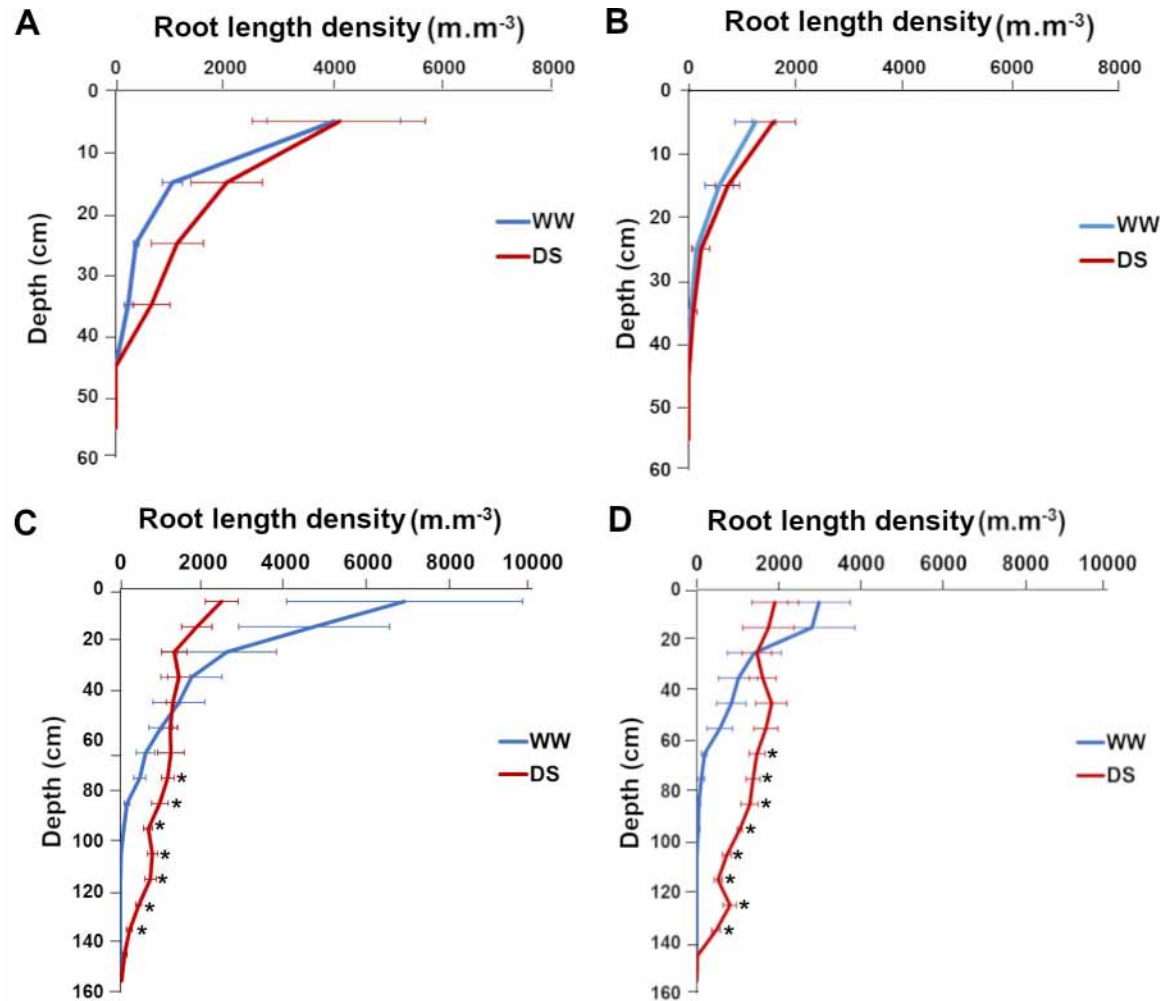
Fig 7. Impact of water deficit on root length density distribution according to depth in SL28 and LCICMB1. SL28 at 43 DAS (A), and 71 DAS (C), LCICMB1 at 44 DAS (B), and 72 DAS (D). Mean of RLD of four plants per variety was considered for each variety.

https://doi.org/10.1371/journal.pone.0214182.g007

However, 31 days after stress application (71 DAS), we observed strong and significant changes in RLD profiles between well-watered and drought stressed plants (Fig 7C and 7D). For both SL28 and LCICMB1, drought stress led to a significant reduction of RLD in the 0–20 cm soil horizon and to a significant increase in RLD in deep soil layers (> 60 cm; Fig 7C and 7D). We used the Racine 2.1 application [29] to generate 2D maps of RLD from our data. These maps clearly showed a drastic change in root development occurring both in SL28 and LCICMB1 with a reduction of RLD in topsoil layers and a colonization of deeper soil layer under drought as compared to well-watered conditions (Fig 8A and 8B). Hence, our data demonstrate that upon drought conditions, both pearl millet lines reduced root growth in the dry topsoil layers and increased their root growth in deeper soil horizons.

We used our RLD data to estimate the total length of the root system of SL28 and LCICMB1 per plot surface ($m.m^2$) between the soil surface and the root front. Drought stress had contrasted impact on total root length per m^2 in both lines. We observed a strong and significant increase in total root system length in LCICMB1 and a non-significant reduction in total root length in SL28 (Fig 9A). In the water stress treatment, the ratio between total root length
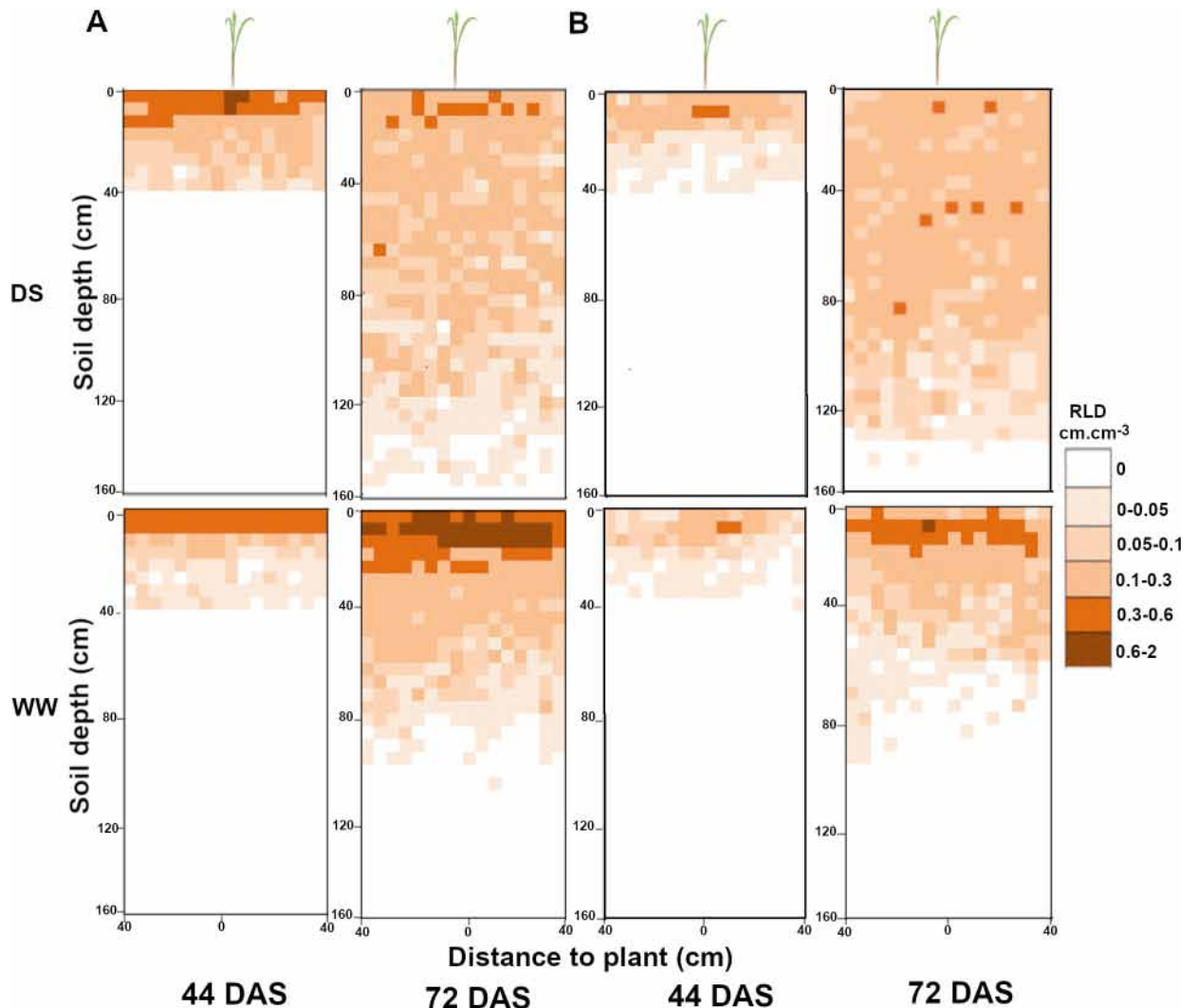
Fig 8. Impact of water deficit on mean root distribution for SL28 and LCICMB1 in the soil profile. Data mapped on a 0.05×0.05 m grid like in the field and expressed in root length density (RLD) in WW and DS conditions for SL28 in (A) and the inbred line LCICMB1 in (B).

https://doi.org/10.1371/journal.pone.0214182.g008

(m.m^{-2}) and shoot biomass (g.m^2) increased in both lines indicating a stronger resource allocation to root growth (Fig 9B). However, this increase was limited and non significant in SL28 while it was large ($>$ 4 times) and significant in LCICMB1 (Fig 9B). Hence, upon drought stress both pearl millet lines seem to reallocate resources to root growth but this reallocation was stronger in LCICMB1.

Discussion

Here, in order to study pearl millet root system in field conditions, we developed a model to estimate root length density (total length of roots per unit of soil volume; RLD) from root intersection densities (i.e., the number of root impacts; RID) on a vertical soil surface (trench). During the development and calibration of the model, we observed that pearl millet root growth orientation was only dependent on soil depth as already observed for other *Poaceae* species [13, 14]. The dependence was particularly important for thick roots ($>$1mm diameter) that should correspond either to the seminal or crown roots [16]. The growth of these roots
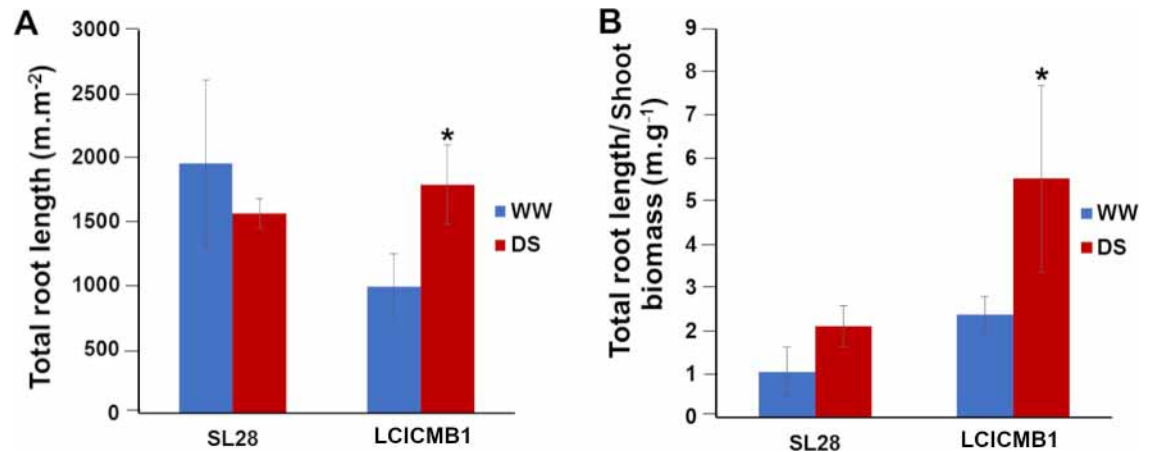
Fig 9. Impact of water deficit on total root length of SL28 and LCICMB1. (A) Total root length (m.m^{-3}) measured at 72 DAS at the end of water stress treatment, and (B) ratio between total root length (m.m^{-3}) and shoot biomass.

was more or less horizontal in shallow soils and became more and more vertical with increased depth. Conversely, the growth orientation of fine roots, which most likely corresponded to the different types of laterals [16,30], was only marginally dependent on soil depth. This led us to develop a model for RLD estimation that considered soil depth as the only variable variable beside RID. This model was validated as the most efficient model to infer RLD from RID. Racine 2.1 [29] was used to manage root data, to calculate RLD and to generate 2D maps of RLD along a soil profile from simple root intersection counts on a vertical plane (trench) thus providing agronomically meaningful information to estimate the efficiency of a root system to acquire water or nutrients in different soil horizons. Like most field root phenotyping methods, this method is not high throughput but allows easy and low-cost analysis of root system response to management practices or environmental factors on a reduced sample of accessions. Our results (RLDs and total root length) are consistent with published data obtained in pearl millet using the very labor-intensive but exhaustive monolith method where the root system of a plant is completely dug up by soil layer [31].

As calibrated here, our model will not be suitable for all areas where pearl millet is grown, and in particular to sites with very different soil composition and organization. However, it was developed on a Dior-type of deep sandy soil that is representative of soils where pearl millet is grown in Sahelian West Africa and validated in different fields to ensure it was robust enough. For very different soil types, our model could be simply re-calibrated by measuring the relation between RLD and RID at different soil depth.

Drought is one of the main factors limiting pearl millet yield and drought episodes are predicted to increase in number and length in the future in West Africa [7, 32]. Previous studies suggested that pearl millet tolerance to dry environments could be due to mechanisms regulating water use efficiency and limiting water loss rather than to improved water acquisition [33]. Interestingly, an expansion of gene families involved in cutin, suberin and wax biosynthesis was observed in pearl millet compared to other cereals and a potential QTL for biomass production under drought was found to co-locate with a gene encoding 3-ketoacyl-CoA synthase that catalyzes the elongation of C24 fatty acids during both wax and suberin biosynthesis [17] thus supporting the link between transpiration barriers and drought resistance in pearl millet. Experiments using lysimeters indicated that temporal patterns of water use, rather than total water uptake, were essential for explaining the terminal drought tolerance of pearl millet genotypes containing a terminal drought tolerance QTL [34]. Therefore, this terminal drought

QTL did not affect the water extraction capacity of the root system. Moreover, it was reported that water stress did not lead to increased water uptake from deep soil suggesting that drought did not lead to a deeper root system [33]. However, the corresponding experiments were performed in pots or lysimeters that limit the full expression of root architecture component compared to field conditions.

We therefore used our phenotyping method to analyze the response of pearl millet root system to water stress during the vegetative phase in field conditions. Our experiments were performed during the dry season on two germplasms with contrasted characteristics: a dual-purpose variety that develops a large aerial biomass and is sensitive to drought and an inbred line with a more limited biomass and that is less sensitive to drought. Our results clearly show that water stress leads to a reallocation of carbon for root growth combined to a reduction of RLD in topsoil layers and to an increase in root system depth. It demonstrates that upon drought stress, pearl millet increases its root growth in deeper soil layer that retain some water. While we cannot conclude from such a small sample, we can hypothesize that this response is adaptive, i.e., that it contributes, with other strategies such as reduction in water loss and temporal regulation of water uptake, to pearl millet tolerance to drought stress. Further work will be needed to test this hypothesis.

In conclusion, we developed a simple way to evaluate and map pearl millet RLD distribution in field conditions. This opens the perspective to characterize the impact of a number of environmental factors and management practices on field-grown pearl millet root system development.

Supporting information

S1 Fig. Climatic data for Exp. 1 & 2.
(PDF)

S2 Fig. Climatic data for Exp. 3.
(PDF)

S3 Fig. Soil water content during Exp. 3.
(PDF)

S1 Table. Typical soil characteristics at the CNRA station (Bambey, Senegal).
(DOCX)

S2 Table. Student t-test on the effect of different factors on the preferential orientation indices (P) of fine (P_f), thick (P_t) and all roots (P_a).
(DOCX)

S1 Dataset. Data from all the experiments.
(XLSX)

Acknowledgments

Author Contributions

Conceptualization: Awa Faye, Bassirou Sine, Jean-Louis Chopart, Alexandre Grondin, Abdala Gamby Diedhiou, Pascal Gantet, Laurent Cournac, Doohong Min, Alain Audebert, Abou-bacry Kane, Laurent Laplaze.

References

1. Burgarella C, Cubry P, Kane NA, Varshney RK, Mariac C, Liu X, et al. A western Sahara centre of domestication inferred from pearl millet genomes. Nat Ecol Evol. 2018; 2: 1377–80. https://doi.org/10.1038/s41559-018-0643-y PMID: 30082736

2. Yadav OP, Singh DV, Vadez V, Gupta SK, Rajpurohit BS, Shekhawat PS. Improving pearl millet for drought tolerance–Retrospect and prospects. Indian J Genet Plant Breed. 2017; 77: 464.

3. Anuradha N, Satyavathi CT, Bharadwaj C, Sankar M, Pathy L. Association of agronomic traits and micronutrients in pearl millet. Int J Chem Stud. 2018; 6: 181–184.

4. Varshney RK, Shi C, Thudi M, Mariac C, Wallace J, Qi P, et al. Pearl millet genome sequence provides a resource to improve agronomic traits in arid environments. Nat Biotech. 2017; 35: 969–976.

5. Garg BK, Kathju S, Lahiri AN. Effect of plant density and soil fertility on pearl millet under drought and good rainfall situations. Ann Arid Zone. 1993; 32: 13–20.

6. Singh P, Boote KJ, Kadiyala MDM, Nedumaran S, Gupta SK, Srinivas K, et al. An assessment of yield gains under climate change due to genetic modification of pearl millet. Sci Total Environ. 2017; 602:1226–37.

7. Vadez V, Hash T, Bidinger FR, Kholova J. II.1.5 Phenotyping pearl millet for adaptation to drought. Front Physiol. 2012; 3: 386. https://doi.org/10.3389/fphys.2012.00386 PMID: 23091462

8. Debieu M, Kanfany G, Laplaze L. Pearl millet genome: Lessons from a tough crop. Trends Plant Sci. 2017; 22: 911–3. https://doi.org/10.1016/j.tplants.2017.09.006 PMID: 28939172

9. Bidinger FR, Hash CTs. Pearl millet. In: Nguyen HT, Blum A, editors. Physiology and Biotechnology Integration for Plant Breeding. New York: Marcel Dekker; 2003. pp. 225–270.

10. Barber SA. Effect of tillage practice on corn (*Zea mays* L.) Root Distribution and Morphology 1. Agron J. 1971; 63: 724–726.

11. Gardner WR. Dynamic aspects of water availability to plants. Soil Sci. 1960; 89: 63–73.

12. Gardner WR. Relation of root distribution to water uptake and availability 1. Agron J. 1964; 56: 41–5.

13. Chopart JL, Siband P. Development and validation of a model to describe root length density of maize from root counts on soil profiles. Plant Soil. 1999; 214: 61–74.

14. Chopart J-L, Rodrigues SR, Carvalho de Azevedo M, de Conti Medina C. Estimating sugarcane root length density through root mapping and orientation modelling. Plant Soil. 2008; 313: 101–12.

15. Chopart J-L, Sine B, Dao A, Muller B. Root orientation of four sorghum cultivars: application to estimate root length density from root counts in soil profiles. Plant Root 2008; 2: 67–75. https://doi.org/10.3117/plantroot.2.67

16. Passot S, Gnacko F, Moukouanga D, Lucas M, Guyomarc'h S, Ortega BM, et al. Characterization of pearl millet root architecture and anatomy reveals three types of lateral roots. Front Plant Sci. 2016; 7: 829. https://doi.org/10.3389/fpls.2016.00829 PMID: 27379124

17. Debieu M, Sine B, Passot S, Grondin A, Akata E, Gangashetty P, et al. Response to early drought stress and identification of QTLs controlling biomass production under drought in pearl millet. PLoS One. 2018; 13: e0201635. https://doi.org/10.1371/journal.pone.0201635 PMID: 30359386

18. Chopart JL, Vauclin M. Water balance estimation model: field test and sensitivity analysis. Soil Sci Soc Am J. 1990; 54: 1377–84.

19. Sinclair T, Ludlow M. Influence of soil water supply on the plant water balance of four tropical grain legumes. Funct Plant Biol. 1986; 13: 329.

20. Tennant D. A test of a modified line intersect method of estimating root length. J Ecol. 1975; 63: 995–1001.

21. Dusserre J, Audebert A, Radanielson A, Chopart J-L. Towards a simple generic model for upland rice root length density estimation from root intersections on soil profile. Plant Soil. 2009; 325: 277.

22. Bohm W. *In situ* estimation of root length density at natural soil profiles. J Agric Sci. 1976; 87: 365–368.

23. Azevedo MCB de, Chopart JL, Medina C de C. Sugarcane root length density and distribution from root intersection counting on a trench-profile. Scientia Agricola. 2011; 68: 94–101.

24. Lang ARG, Melhuish FM. Lengths and diameters of plant roots in non-random populations by analysis of plane surfaces. Biometrics. 1970; 26: 421.

25. Van Noordwijk M. Method for quantification of root distribution patterns and root dynamics in the field. In: Methodology in soil-K research: proceedings of the 20th Symposium of the International Potash Institute Bern: International Potash Institute; 1987. pp 247–256

26. Nash JE, Sutcliffe JV. River flow forecasting through conceptual models part I—A discussion of principles. J Hydrol (Amst). 1970; 10: 282–290.

27. Loague K, Green RE. Statistical and graphical methods for evaluating solute transport models: Overview and application. J Contam Hydrol. 1991; 7: 51–73.

28. Willmott CJ, Robeson SM, Matsuura K. A refined index of model performance. Int J Climatol. 2012; 32: 2088–94.

29. Chopart JL, Faye A, Lindemann J, Mézino M, RACINE2.2: Application de gestion de calculs et de cartographie de données racinaires obtenues à partir de comptages de racines sur des profils de sol. Version 2.2 Notice d'utilisation (2019): 18.

30. Passot S, Moreno-Ortega B, Moukouanga D, Balsera C, Guyomarc'h S, Lucas M, et al. A new phenotyping pipeline reveals three types of lateral roots and a random branching pattern in two cereals. Plant Physiol. 2018; 177: 896–910. https://doi.org/10.1104/pp.17.01648 PMID: 29752308

31. Chopart J. L. Etude du système racinaire du mil (*Pennisetum typhoides*) dans un sol sableux du Sénégal. L'Agronomie Tropicale. 1975; 38: 37–51.

32. Ben Mohamed A, van Duivenbooden N, Abdoussallam S. Impact of climate change on agricultural production in the Sahel–Part 1. Methodological approach and case study for millet in Niger. Clim Change. 2002; 54: 327–348.

33. Zegada-Lizarazu W, Iijima M. Deep root water uptake ability and water use efficiency of pearl millet in comparison to other millet species. Plant Prod Sci. 2005; 8: 454–460.

34. Vadez V, Kholová J, Yadav RS, Hash CT. Small temporal differences in water uptake among varieties of pearl millet (*Pennisetum glaucum* (L.) R. Br.) are critical for grain yield under terminal drought. Plant Soil. 2013; 371: 447–462.